

PAPER • OPEN ACCESS

Hot corrosion behavior of $\text{Yb}_2\text{Si}_2\text{O}_7$ ceramic by NaVO_3 and V_2O_5 at 700° to 900°

To cite this article: Yongqiu Zhang *et al* 2019 *IOP Conf. Ser.: Mater. Sci. Eng.* **563** 022022

View the [article online](#) for updates and enhancements.

Hot corrosion behavior of $\text{Yb}_2\text{Si}_2\text{O}_7$ ceramic by NaVO_3 and V_2O_5 at 700°C to 900°C

Yongqiu Zhang¹, Daqian Sun¹, Zhenan Ren^{1*}, Binglin Zou²

¹Key Laboratory of Automobile Materials, School of Materials Science and Engineering, Jilin University, Changchun 130025, PR China

²State Key Laboratory of Rare Earth Resources Utilization, Changchun Institute of Applied Chemistry, Chinese Academy of Sciences, Changchun 130022, Jilin, China

Corresponding author's e-mail: rza@jlu.edu.cn

Abstract. To better understand the hot corrosion behavior of $\text{Yb}_2\text{Si}_2\text{O}_7$ ceramic in molten NaVO_3 and V_2O_5 , corrosion experiments were performed using sintered $\text{Yb}_2\text{Si}_2\text{O}_7$ bulk ceramics with NaVO_3 and V_2O_5 coatings at temperature range of 700°C to 900°C in air. Corrosion products of YbVO_4 and SiO_2 were identified under NaVO_3 corrosion. But only YbVO_4 was found under V_2O_5 corrosion with some residual corrosion agent. In above two conditions, the corrosion products of YbVO_4 have the same crystallographic structural characteristic, but morphology has significant difference. In the first case, YbVO_4 is rod-like with a tetrahedral cone at each end because of NaVO_3 being weak acid to lead to lower driving force for the corrosion reactions. Thus corrosion products of YbVO_4 grew with less nuclei and large elongation. However, V_2O_5 showed strong acid with strong driving force bringing higher nucleation rate and suppressing the growth of YbVO_4 , which resulted in granular YbVO_4 . And the size of granular YbVO_4 crystals increased slightly with test temperature rising.

1. Introduction

Si-based ceramics, such as SiC and Si_3N_4 , can be used as high temperature structural components for aeroengine. Under dry oxygen conditions, a layer of SiO_2 protective layer will be formed on the surface of Si-based ceramics, showing good oxidation resistance [1]. However, the water vapor in the high temperature gas reacts with the SiO_2 protective layer to form the gaseous product $\text{Si}(\text{OH})_4$, which results in the decrease of the high temperature performance of the ceramic components. Therefore, environmental barrier coatings (EBCs) are often used to prevent the formation of $\text{Si}(\text{OH})_4$ and improve their service life [2-4]. Rare earth silicates have good chemical stability, oxidation resistance, chemical compatibility with Si-based ceramics and water-oxygen corrosion resistance [5-7]. They are the most promising candidate materials for EBCs.

Among rare earth silicates, $\text{Yb}_2\text{Si}_2\text{O}_7$ has good phase stability from room temperature to high temperature, matching thermal expansion coefficient with SiC and better resistance to water-oxygen corrosion [5, 8]. However, in addition to a large amount of water vapor, oxygen and siliceous minerals, there are also various molten salt impurities (such as Na, S, V, Cl, etc.) in the exhaust gas of aeroengine, which can cause corrosion of substrates and EBCs of high temperature components [9-12]. It is necessary to study the corrosion behavior of NaVO_3 and V_2O_5 molten salts on $\text{Yb}_2\text{Si}_2\text{O}_7$ ceramic.



2. Materials and methods

In order to simulate the molten salt corrosion condition of EBCs, $\text{Yb}_2\text{Si}_2\text{O}_7$ sintered bulk ceramics were used as corrosion specimen. Its powders were synthesized by using commercial Yb_2O_3 and SiO_2 powders (purities > 99%) at 1500°C . The chemical reaction formula is shown in chemical equation (1). $\text{Yb}_2\text{Si}_2\text{O}_7$ powders were weighed 5 g and put into a press die. And its compacts with the size of $15\text{ mm} \times 15\text{ mm} \times 6.5\text{ mm}$ were prepared by using a single-axis hydraulic press under 20 MPa pressure for 5 min. When sintered in a box furnace at 1500°C for 12 hours, the size of the sintered bulk ceramics is $12.2\text{ mm} \times 12.2\text{ mm} \times 4.5\text{ mm}$. Their macroscopic surface is relatively smooth. The $\text{Yb}_2\text{Si}_2\text{O}_7$ equiaxed grains are compactly accumulated and the grain boundary is clear^[13], but there are a few small pores at the grain boundary. The surface morphology is shown in Fig. 1. The results of XRD showed that both $\text{Yb}_2\text{Si}_2\text{O}_7$ powders and the sintered bulk ceramics were pure $\text{Yb}_2\text{Si}_2\text{O}_7$ phase.

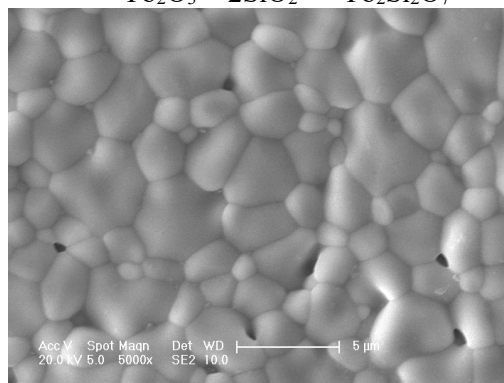


Fig.1. SEM image of the surface of sintered $\text{Yb}_2\text{Si}_2\text{O}_7$ ceramic bulk

The temperature range of gas emitted by aeroengine is large. In this paper, the temperature range of 700°C - 900°C was chosen as the test condition with holding time of 2 hours. The corrosive media of NaVO_3 and V_2O_5 powders were uniformly coated on the upper surface of the $\text{Yb}_2\text{Si}_2\text{O}_7$ ceramic specimens at a concentration of about 20 mg/cm^2 . Then hot corrosion tests were carried out by putting these corrosive samples into the box furnace at a set temperature of 700°C , 800°C or 900°C . After corrosion test, the corroded samples were taken out and naturally cooled to room temperature.

The corroded samples were cleaned with deionized water and their phase components were identified by X-ray diffraction (XRD, Bruker D8 Advance diffractometer, Cu K radiation) at a scanning rate of $6^\circ/\text{min}$. The microstructures were observed by scanning electron microscopy (SEM, JSM-5310, Japan) equipped with an energy-dispersive X-ray spectrometer (EDS, Link-ISIS, England) operating at 20 KV.

3. Results

Fig. 2 shows XRD analysis results of $\text{Yb}_2\text{Si}_2\text{O}_7$ bulk ceramics. As can be seen from Fig. 2a, the samples coated NaVO_3 powders have diffraction peaks of yttrium vanadate (YbVO_4) and silicon dioxide (SiO_2) in addition to $\text{Yb}_2\text{Si}_2\text{O}_7$ after corrosion, but NaVO_3 phase is not detected, and the influence of temperature change on XRD diffraction peaks is not evident. Fig. 2b is the XRD analysis results after the samples were corroded by V_2O_5 coating. YbVO_4 diffraction peaks appeared at all test temperatures. V_2O_5 phase remained in samples at 700°C and 800°C , while it was not detected after 900°C corrosion, indicating that corrosive agent was consumed.

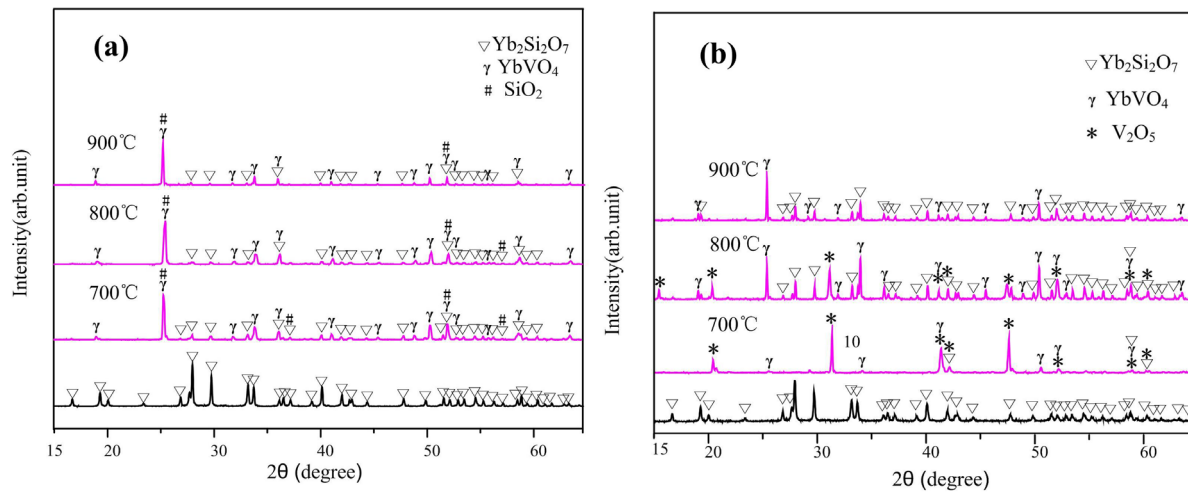


Fig.2. XRD patterns of $\text{Yb}_2\text{Si}_2\text{O}_7$ corroded samples with NaVO_3 coating (a) and V_2O_5 coating (b) before hot corrosion

The SEM images of the corroded sample surfaces are shown in Fig. 3(a), (b) and (c) which were obtained at 700°C, 800°C and 900°C respectively by coating NaVO_3 before hot corrosion. Two kinds of corroded products are observed with different morphology marked A and B in Fig. 3(a). The shape of the product A is rod with a tetrahedral cone at each end, while the product B is lamellar agglomeration. Also, the elemental compositions of A and B corroded products are different by EDS analyses and they were mainly composed by Yb, V and O at point A and Si and O at point B. After comprehensively analyzing with XRD results, the corroded products at A and B were identified as YbVO_4 and SiO_2 respectively.

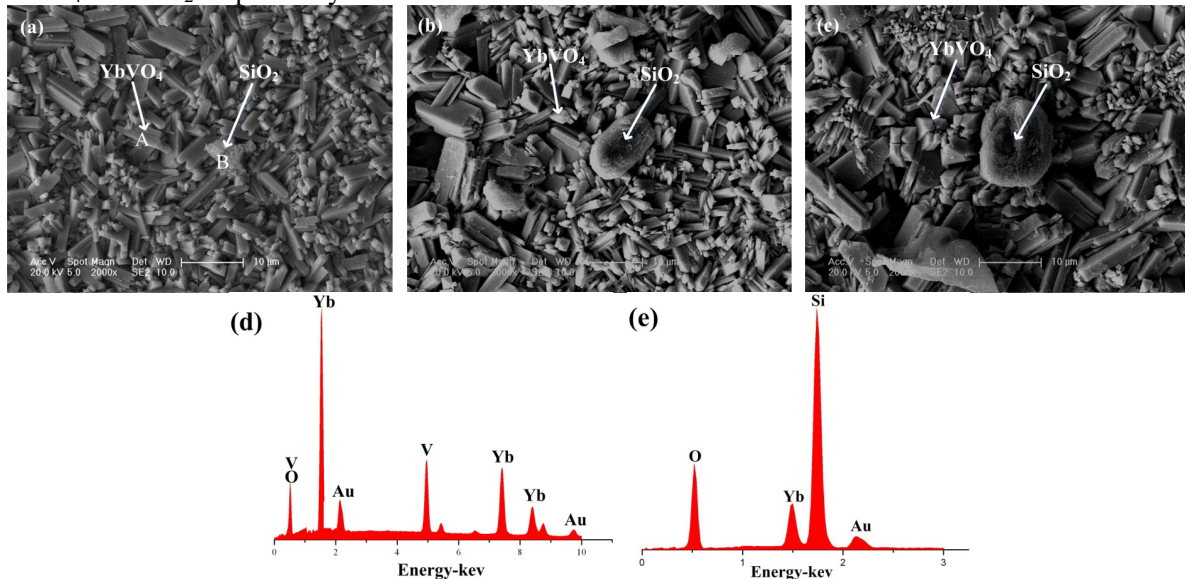


Fig. 3 The SEM images of the corroded sample surfaces obtained at 700°C (a), 800°C (b) and 900°C (c) respectively by coating NaVO_3 before hot corrosion and the EDS analysis results at point A (d) and B (e)

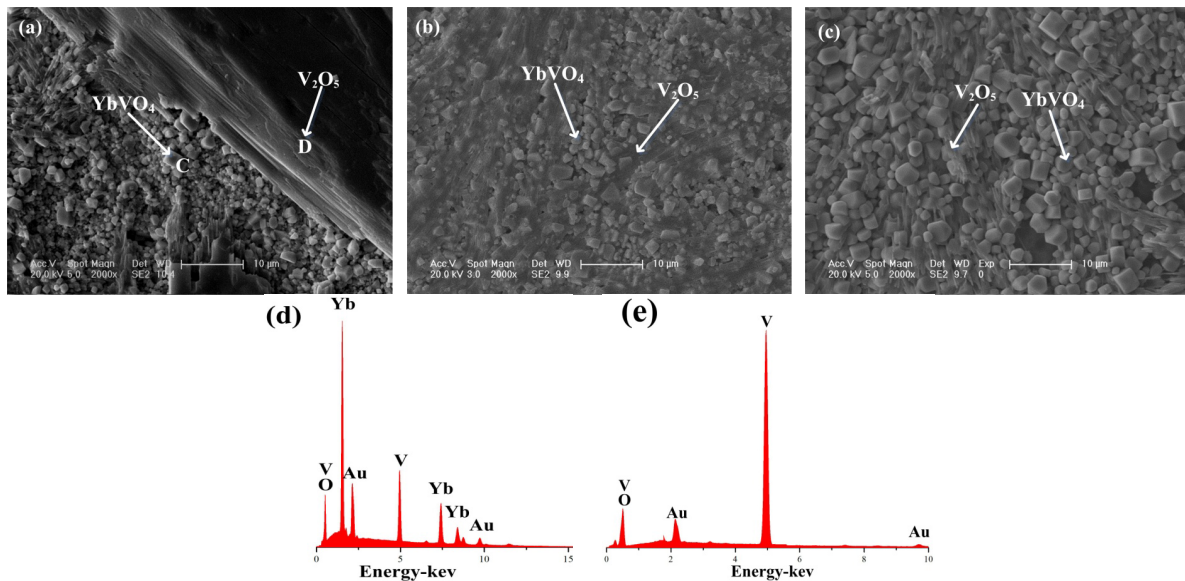


Fig. 4 The SEM images of the corroded sample surfaces obtained at 700°C (a), 800°C (b) and 900°C (c) respectively by coating V_2O_5 before hot corrosion and the EDS analysis results at point C (d) and D (e)

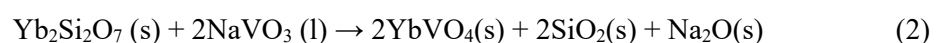
From the SEM images in Fig. 3(a), (b) and (c), the morphology changes of the corroded products $YbVO_4$ and SiO_2 are clearly different. The shape and size of $YbVO_4$ hardly changed with hot corrosion temperatures. While the morphology of SiO_2 agglomeration changed from lamellar at 700°C to bigger axiolitic at 800°C and then much bigger at 900°C.

Unlike the analysis results in Fig. 3, only $YbVO_4$ was obtained by coating V_2O_5 on $Yb_2Si_2O_7$ bulk ceramics at 700°C to 900°C and its shape was granular. From the images of Fig. 4 (a), (b) and (c), it can be seen that the size of $YbVO_4$ grains increased slightly with increasing test temperatures. Moreover, the V_2O_5 on the surface of the samples left more and thicker at 700°C, and the less residual V_2O_5 was in the form of a thin fluid after corrosion at 800°C and 900°C.

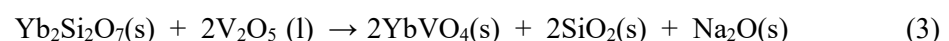
4. Discussion

The hot corrosion mechanism mainly includes the vulcanization and dilution processes [14]. The chemical reaction of vanadium compounds with metal oxides follows a Lewis acid-base dilution mechanism and the acid-base properties of metal oxides depend on the acidity and alkalinity of the reactants [15]. The acid-base dilution mechanism is widely used in ceramic materials. For example, the reaction of YSZ and Ti_3SiC_2 can be explained by this theory [16,17]. According to this theory, $Yb_2Si_2O_7$ can be regarded as composed of Yb_2O_3 and SiO_2 in a ratio of 2:1, wherein SiO_2 is an acidic oxide, and the acidity or alkalinity of the metal oxide Yb_2O_3 mainly depends on the acid-base property of the molten salt.

For the weakly acidic $NaVO_3$, the corrosion product of $YbVO_4$ composed at 700°C to 900°C, is due to the reaction of acidic salt with Yb_2O_3 . Therefore, the corrosion mechanism in that case can be described by the chemical equation (2).



For strong acidic V_2O_5 , the corrosion mechanism at 700°C to 900°C can be described by the chemical equation (3).



As shown in Fig. 3 and Fig. 4, the corrosion product of $YbVO_4$ exhibited significant different

morphology. The crystal structure of YbVO_4 was reported to be similar to that of ZrO_2 [18, 19]. The growth mode of the YbVO_4 crystal having the ZrO_2 structure is a tetragonal prism and a tetragonal double-cone type, it is the reason why the YbVO_4 generated by the NaVO_3 corrosion reaction is a rod shape with pyramids at both ends. The crystal of YbVO_4 preferentially grows in the c-axis (0 0 1) direction as shown in Fig.5. However, according to research reports, the main driving force for crystal growth and morphological change is the reduction of surface energy. The order of the free energy of the ZrO_2 crystal plane is $(0\ 0\ 1) < (1\ 1\ 0) < (1\ 1\ 2)$ [20]. At the same time, Chen and Rosenflanz [21] pointed out that driving force is essential for crystal elongation. Lower driving force leads to less nucleation rate and the possibility of crystal elongation is greater. Conversely, the greater the driving force, the higher the nucleation rate. So the possibility of crystal elongation is less. Under experimental conditions, the acidity of V_2O_5 is stronger than that of NaVO_3 and the driving force of the reaction is greater. Thus a large amount of crystallization nuclei will occur and a high nucleation rate will inhibit the growth of YbVO_4 crystal. Finally, granular YbVO_4 crystal are obtained. For the latter, only rod-like corrosion product of YbVO_4 can be obtained.

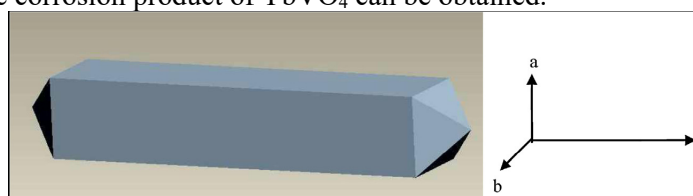


Fig.5. Schematic diagram of the morphology of YbVO_4 crystal obtained on surface of $\text{Yb}_2\text{Si}_2\text{O}_7$ bulk ceramics coated by NaVO_3 [20]

5. Conclusions

(1) The corrosion reaction at 700°C to 900°C for $\text{Yb}_2\text{Si}_2\text{O}_7$ bulk ceramics coated with NaVO_3 led to products of YbVO_4 and SiO_2 and their morphology were rod-shaped with tetrahedral pyramid at both ends and lamellar to axiolitic agglomeration, respectively.

(2) When $\text{Yb}_2\text{Si}_2\text{O}_7$ bulk ceramics were corroded by V_2O_5 at 700°C to 900°C , the morphology of corrosion product YbVO_4 was granular and its crystal size increased with the temperature rising. There was some V_2O_5 left on the surface of the $\text{Yb}_2\text{Si}_2\text{O}_7$ bulk ceramics.

(3) Under the experimental conditions, less crystal growth driving force resulted in lower nucleation rate for corrosion product YbVO_4 because the corrosion agent NaVO_3 shows weak acidic. So rod-like YbVO_4 was obtained and its size hardly changed. But strong acidic V_2O_5 led to greater crystal growth driving force. The nucleation rate of corrosion product YbVO_4 was higher and its shape changed to granular. The size of granular YbVO_4 increased with temperature rising, but the number decreased.

Acknowledgement

This work was supported by National Natural Science Foundations of China (NSFC 51472235).

References

- [1] N S Jacobson, D S Fox, E J Opola. High temperature oxidation of ceramic matrix composites [J]. Pure and Applied Chemistry, 1998, 70(2): 493-500.
- [2] K.N. Lee. Current status of environmental barrier coatings for Si-based ceramics [J]. Surface & Coating Technology, 2000, 133-134:1-7.
- [3] H E Eaton, G D Linsey. Accelerated oxidation of SiC CMC's by water vapor and protection via environmental barrier coating approach [J]. Journal of the European Ceramic Society, 2002, 22(14-15): 2741-2747.
- [4] S Ueno, T Ohji, H T Lin. Designing lutetium silicate environmental barrier coatings for silicon nitride and its recession behavior in steam jets [J]. Journal of Ceramic Processing Research, 2006, 7(1): 20-23.

- [5] Y. Wang, J. Liu. First-principles investigation on the corrosion resistance of rare earth disilicates in water vapor [J]. *Journal of the European Ceramic Society*, 2009, 29 (11): 2163-2167.
- [6] K.N. Lee, D.S. Fox, N.P. Bansal. Rare earth silicate environmental barrier coatings for SiC/SiC composites and Si₃N₄ ceramics [J]. *Journal of the European Ceramic Society*, 2005, 25(10): 1705-1715.
- [7] S. Ueno, D.D. Jayaseelan, N. Kondo, T. Ohji, S. Kanzaki, H.T. Lin. Development of EBC for silicon nitride [J]. *Key Engineering Materials*, 2005, 287:449-456.
- [8] N. Maier, K.G. Nickel, G. Rixecker. High temperature water vapor corrosion of rare earth disilicates (Y, Yb, Lu)₂Si₂O₇ in the presence of Al(OH)₃ impurities [J]. *Journal of the European Ceramic Society*, 2007, 27(7): 2705-2713.
- [9] N S Jacobson, Corrosion of silicon-based ceramics in combustion environments [J]. *Journal of the American Ceramic Society*, 1993, 76(1): 3-28.
- [10] N S Jacobson, J L Smialek. Hot corrosion of sintered a-SiC at 1000°C [J]. *Journal of the American Ceramic Society*, 1985, 68(8): 432-439.
- [11] N S Jacobson. Kinetics and mechanism of corrosion of SiC by molten salts [J]. *Journal of the American Ceramic Society*, 1986, 69(1): 74-82.
- [12] K.L. Luthra, H.S. Spacil. Impurity deposits in gas-turbines from fuels containing sodium and vanadium [J]. *Journal of The Electrochemical. Society*, 1982, 129(3): 649-656.
- [13] Z. L. Tian, L. Y. Zheng, J. M. Wang, J. B. Yang, G. Yang, J. Y. Wang. Damage tolerance and extensive plastic deformation of β -Yb₂Si₂O₇ from room to high temperatures [J]. *Journal of the American Ceramic Society*, 2015, 98(9): 2843-2851.
- [14] R. A. Rapp. Hot corrosion of materials: a flexing mechanism [J]. *Corrosion Science*, 2002, 44(2): 209-221.
- [15] Z. H. Xu, L. M. He, R. D. Mu, S. M. He, G. H. Huang, X. Q. Cao. Hot corrosion behavior of rare earth zirconates and yttriapartially stabilized zirconia thermal barrier coatings [J]. *Surface & Coatings, Technology*, 2010, 204(21-22): 3652-3661.
- [16] C. Lens, I. G. Wright, B. A. Pint. Hot corrosion of an EB-PVD thermal barrier coating system at 950°C [J]. *Oxidation of Metals*, 2000, 54(5-6): 401-424.
- [17] G. M. Liu, M. S. Li, Y. C. Zhou. Effect of Na₂SO₄ and water vapor on the corrosion of Ti₃SiC₂ [J]. *Oxidation of Metals*, 2006, 66(1-2): 115-125.
- [18] Y.G. Yu, Y. Cheng, H.J. Zhang, J.Y. Wang, X.F. Cheng, H.R. Xia. Growth and thermal properties of YbVO₄ single crystal [J]. *Materials Letters*, 2006, 60: 1014-1018.
- [19] H.J. Zhang, Y.G. Yu, Y. Cheng, J.H. Liu, H.X. Li, W.W. Ge, et al. Growth of YbVO₄ stoichiometric crystal [J]. *Journal of Crystal Growth*, 2005, 283(3-4): 438-443.
- [20] Sa Li, Zhan-Guo Liu, Jia-Hu Ouyang. Growth of YbVO₄ crystals evolved from hot corrosion reactions of Yb₂Zr₂O₇ against V₂O₅ and Na₂SO₄ + V₂O₅ [J]. *Applied Surface Science*, 2013, 276: 653- 659.
- [21] I.W. Chen, A. Rosenflanz. A tough SiAlON ceramic based on α -Si₃N₄ with a whisker-like microstructure [J]. *Nature*, 1997, 389(6652): 701-704.